View metadata, citation and similar papers at core.ac.uk
brought to you by CORE
provided by University of Bath Research Portal

Citation for published version:
Mohammadi, A, Karmakar, NC & Yuce, MR 2016, 'Post-fabrication selective magnetic annealing technique in standard MEMS processes', Applied Physics Letters, vol. 109, no. 22, 221906.
https://doi.org/10.1063/1.4971262

DOI:
10.1063/1.4971262

Publication date:
2016

Document Version
Publisher's PDF, also known as Version of record

Link to publication

University of Bath

General rights
Copyright and moral rights for the publications made accessible in the public portal are retained by the authors and/or other copyright owners and it is a condition of accessing publications that users recognise and abide by the legal requirements associated with these rights.

Take down policy
If you believe that this document breaches copyright please contact us providing details, and we will remove access to the work immediately and investigate your claim.

Download date: 13. May. 2019

.

A post-fabrication selective magnetic annealing technique in standard MEMS processes

A. Mohammadi, N. C. Karmakar, and M. R. Yuce

Citation: Appl. Phys. Lett. **109**, 221906 (2016); doi: 10.1063/1.4971262
View online: http://dx.doi.org/10.1063/1.4971262
View Table of Contents: http://aip.scitation.org/toc/apl/109/22
Published by the American Institute of Physics

RIGHTSLINK
Copyright Clearance Center

CrossMark click for updates

A post-fabrication selective magnetic annealing technique in standard MEMS processes

A. Mohammadi,[1,a)] N. C. Karmakar,[2] and M. R. Yuce[2]
[1]*Engineering Science, University of Oxford, Parks Road, Oxford OX1 3PJ, United Kingdom*
[2]*Electrical and Computer Systems Engineering, Monash University, Clayton, VIC 3800, Australia*

(Received 2 August 2016; accepted 18 November 2016; published online 1 December 2016)

A selective electrothermal magnetic annealing technique is introduced that provides programming capabilities for mechanical micro-resonators. In the proposed approach, the magnetic properties of resonators can be locally tuned in a post-fabrication batch-compatible process step. A prototype is implemented in a standard microfabrication process, where resonating ferromagnetic elements are suspended on top of a polysilicon resistive heater. The ferromagnetic elements consist of electroplated Nickel (Ni) with minor Iron (Fe) impurities. The electro-thermo-mechanical heating phenomenon is simulated for design purposes. The magnetization of micro-resonators with and without magnetic annealing is measured. The resulting magnetic property enhancement is illustrated by hysteresis (M-H) loop variations. *Published by AIP Publishing*. [http://dx.doi.org/10.1063/1.4971262]

Compared with other mechanisms, the magnetic transduction demonstrates a superior performance in several perspectives. Batch fabrication of magnetic micro-devices is under intense investigation for niche applications in sensors, actuators, energy harvesting devices, etc. The ongoing research is mainly focused on the integration of magnetic materials in standard fabrication processes for micro/nano-electromechanical systems (M/NEMS).[1,2] Electrodeposition, laser ablation, molecular beam epitaxy, and sputter deposition are highly developed for implementing ferromagnetic layers in micro/nano-fabrication processes.[1,3] Several approaches have been introduced for tuning the magnetic properties of ferromagnetic layers in nano/micro-devices.[4–6] However, the magnetic properties adopted by these layers during the microfabrication process are hardly changeable afterwards and they feature identical magnetic properties. In the literature, no post-processing batch-compatible technique is reported for the selective tailoring of magnetic attributes of each component.

We introduce an integrated local tuning technique of magnetic properties for ferromagnetic micro-machined resonators. The goal is to develop a magnetic platform for mechanical memories.[7,8] Example applications include magnetomechanical elements for radio frequency identification (RFID) in harsh environments.[9] In this application, electromagnetic waves from a transponder interrogate the microresonator elements, whose response is measured by the transponder pick-up coil.[8] The response depends on the Lorentz force applied to the resonator, which is determined by the physical attributes of individual elements including mechanical and magnetic features. Magnetization has a high programmability potential for microdevices among the other features. The mechanical force (F) applied from transponder to the magnetic dipole (resonator) is related to its magnetization (M) by the following equation:

$$F = \mu_0 \nu M \nabla H, \tag{1}$$

where μ_0, ν, ∇, and H are the permeability of free space, the volume of microresonator, the gradient operator, and the applied magnetic field, respectively.[10] In order to create unique resonance signatures, a post-processing technique is desired to tailor the magnetic anisotropy of these elements, so that resonators with/without magnetic annealing can resemble digital ones/zeros, as they respond to an external magnetic field. The proposed magneto-electro-thermal method is capable of selecting a certain resonator for magnetic annealing by means of a local heating structure. A prototype is implemented in an standard microfabrication process to provide a proof of the concept, though the presented technique can be used for programming purposes in other M/NEMS platforms. The selective magnetic annealing technique is described in the below paragraph, followed by the electrothermal modelling approach. For evaluation purposes, the magnetization of the prototype is measured, which is directly related to the force applied to microresonators through Eq. (1). The measured M-H curve of the prototype is described in the last paragraph.

Magnetic anisotropy of a material is a function of its crystal orientation, magneto-elasticity, and shape.[3] The contribution of each factor can be dominant depending on material, fabrication processes, etc. Nonetheless, magnetic annealing, i.e., annealing below the Currie temperature under the influence of an intense external magnetic field, is a commonly accepted method to enhance the anisotropy of ferromagnetic materials. Local temperature control on micromechanical devices is addressed either off-chip by a high power laser beam[11] or on-chip by resistors embedded in the microdevice structure.[12]

By combining local heating and magnetic annealing, we devise a selective annealing method in MEMS. Figure 1 illustrates a schematic view of the proposed platform in MEMS. The micro-resonator device consists of ferromagnetic plates suspended on top of serpentine resistive heaters. Heaters can be etched in a Polysilicon layer and individually connected to the electrical power supply via deposited gold pads. Supplying power to heaters increases their temperature. There is a thin air gap between each heater and the ferromagnetic resonator on top. Heat transfer through the air gap

a)Electronic mail: ali.mohammadi@eng.ox.ac.uk

RIGHTSLINK

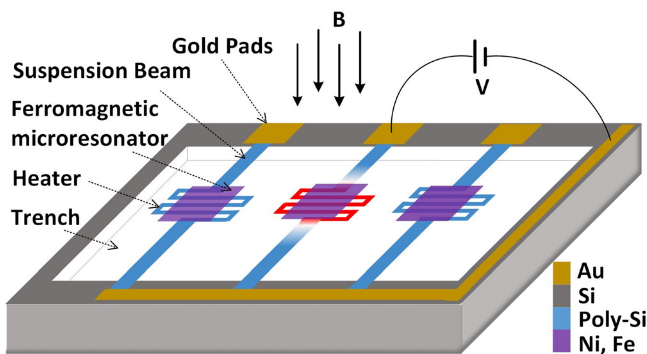

FIG. 1. Proposed structure: three suspended micro-resonators equally exposed to the magnetic field (B) while only one of them is selected by the heater for magnetic annealing.

increases the temperature of its corresponding resonator. Consequently, each resonator can be selected for magnetic annealing by applying electrical power to its corresponding heater, while being exposed to a strong magnetic field. The perpendicular field (B) is supplied externally to the whole chip, though the field makes permanent influences on the selected resonators only (middle resonator in Figure 1).

The prototype is implemented in a standard MEMS fabrication process.[13] The main structural layer is a 20 μm thick electroplated Nickel with Iron impurities, as illustrated in Figure 2. The whole process is built on a silicon substrate and electrically isolated from substrate by a 2 μm oxide layer (SiO_2). A 0.7 μm thick doped Polysilicon layer is encapsulated between two Silicon-Nitride (Si_3N_4) layers for electrical isolation. While anchor metal layer is needed to fix the metal on the substrate, the sacrificial layer is deposited for

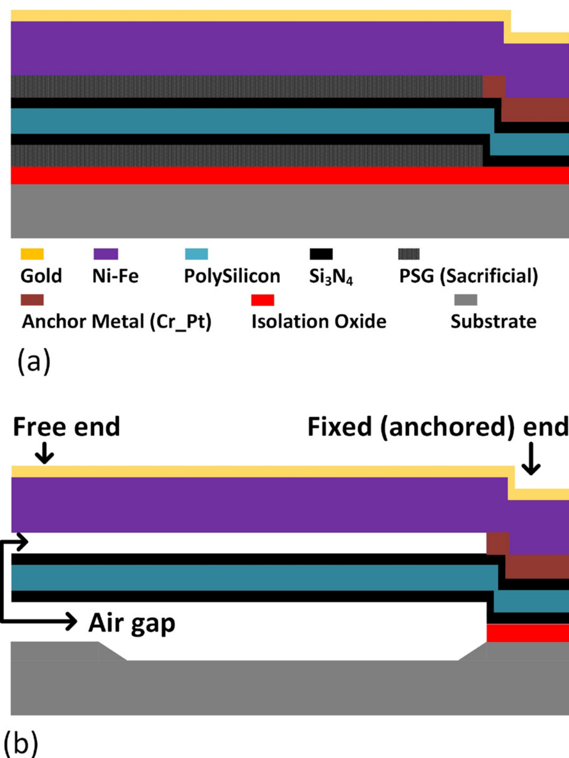

FIG. 2. The cross-sectional view of the last microfabrication process step: (a) all the required layers in the process and (b) etching sacrificial layers and isolation oxide to release the metal and polysilicon.

releasing the metal. As shown in Figure 2(b), a 1.1 μm thin air gap is opened in between metal and Polysilicon after etching. In addition, a 25 μm deep trench is etched away from the substrate to avoid heat dissipation from the heater to substrate. Further details of the microfabrication process are explained in the Metal-MUMP design handbook.[13]

Polysilicon is commonly used as a heater due to its electrical resistance and mechanical properties. A serpentine heater is designed to fit underneath the metal to control its temperature during magnetic annealing process as shown in Figure 1. The suspension beams are designed thicker for mechanical stability, and the serpentine part is thinner for increased electrical resistance and localized temperature control. In order to derive heater dimensions, finite element analysis is needed to model the heat transfer phenomena. The model is typically built based on standard design kits provided by foundries. However, a modification in the technology file is needed here to simulate the heat transfer through the thin air gap between the metal and poly layers. This gap is first filled with sacrificial material (PSG) and then etched away to release the metal at final microfabrication steps. The standard three dimension model leaves an empty gap after the etching process. In order to replace the empty gap with air in the model builder, the etching step is removed from the simulator process steps, and the physical properties of the sacrificial material, such as thermal conduction coefficient, are replaced by air properties. The steady state electro-thermo-mechanical finite element analysis results are shown in Figure 3.

We assume that conduction dominates the heat transfer mechanism, though convection and radiation can also be added. The boundary conditions used for finite element analysis include the fixed room temperature (300°K) and electrical potential difference (0–100 V) at the two ends of the heater suspension beam. In addition, the anchored ends of microresonator are fixed points. The device substrate and isolation oxide are omitted from the model to simplify the design procedure. The metal layer shown in Figure 3(a) is heated up to 350°K while the central part of poly heater, shown in Figure 3(b), is at around 400°K.

Prototype samples are fabricated in standard Metal-MUMPs technology. Figure 4(a) illustrates the tilted SEM image of the sample resonator, which is diced from a 8 mm $\times$ 8 mm chip to fit in the vibrating sample magnetometer (VSM). It consists of a metal plate, suspension beams, and gold pads that connect the heater to voltage power supply via the bonding wires. The Polysilicon heater is hidden underneath the plate; however, its traces are visible on the gold surface in Figure 4(b), which is a plan view of the SEM image. The microfabricated serpentine Polysilicon is a 20 kΩ resistor. Figure 4(b) also shows the planar dimensions of the device from which the metal plate size is 500 μm $\times$ 500 μm.

In the first experiment, the temperature and current are monitored while applying voltage to the heater. The hot plate temperature is measured by a thermocouple as illustrated in Figure 5. It should be noted that the simulated model represents the steady state spatial distribution of temperature in response to 100 V input voltage while in the experimental setup, after increasing each voltage step, it takes a few seconds up to less than a minute for the plate to reach an

RIGHTSLINK

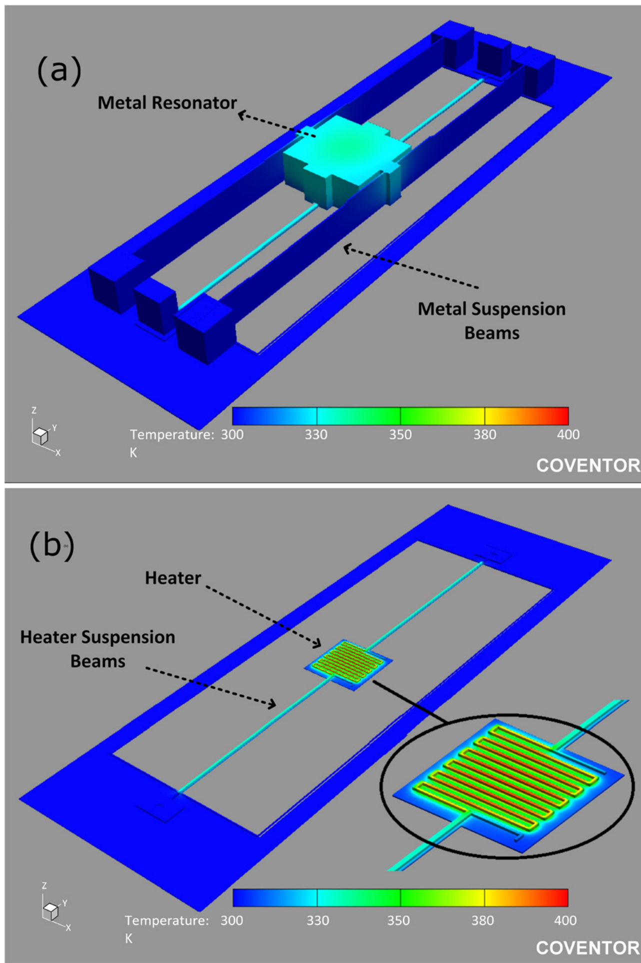

FIG. 3. The slices of the device model for steady state temperature distribution after electrothermal heating: (a) metal top and (b) Polysilicon heater.

equilibrium with room temperature. Though the measurement result at 100 V input voltage is in good agreement with the simulation results shown in Figure 3. The measured temperature from metal surface (52 °C) at 100 V corresponds to 330°K in simulation (Figure 3(b)), considering the fact that in simulation the room temperature effect is ignored. The maximum temperature in Figure 3(b) is 400°K due to the Polysilicon heater, which is inaccessible for thermocouple measurement. Further increase in the applied voltage expands the volume of heater so that it touches the bottom side of resonator plate and fuses from the beam arms as it is observable under microscope.

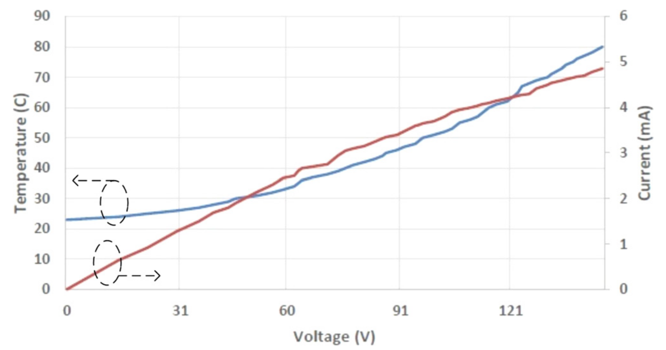

FIG. 5. Plate temperature and heater current versus applied voltage.

In the next step, samples are located in between two strong permanent magnets to apply a perpendicular magnetic field while connected to the maximum voltage for an hour. Magnetization of the chips with and without annealing process is measured at the same direction. A high precision vibrating sample magnetometer (VSM) built in a Quantum Design Physical Property Measurement System (PPMS model 6000) is used for the evaluation purpose. VSM is operated at 40 Hz with 2 mm displacement amplitude. The magnetization versus applied field curve (hysteresis loop) is shown in Figure 6, which is obtained in 300°K by applying the magnetic field ramped at 20 Oe/s. The increased coercivity shows a higher saturation for a certain magnetic field density, which approves the desired permanent change in anisotropy.

Implementation of the proposed magnetic programming technique in a standard microfabrication process demonstrates its superior reliability. However, higher magnetization could be achieved by using an accurate percentage of Iron in

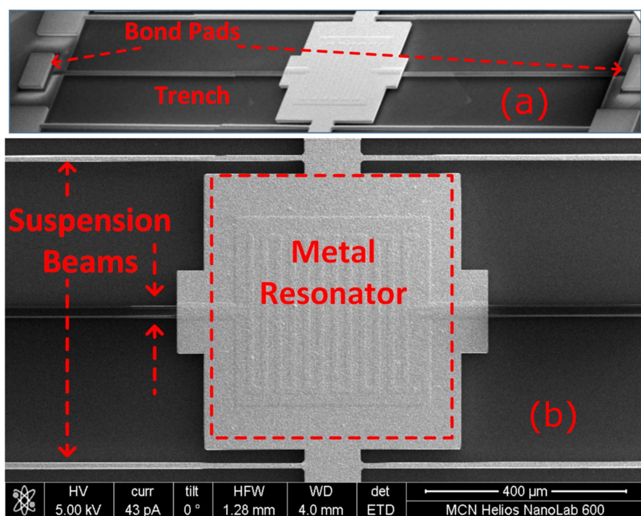

FIG. 4. The SEM image of the MEMS device: (a) tilted view of the whole device and (b) zoom on plan view shows the Polysilicon traces on metal surface.

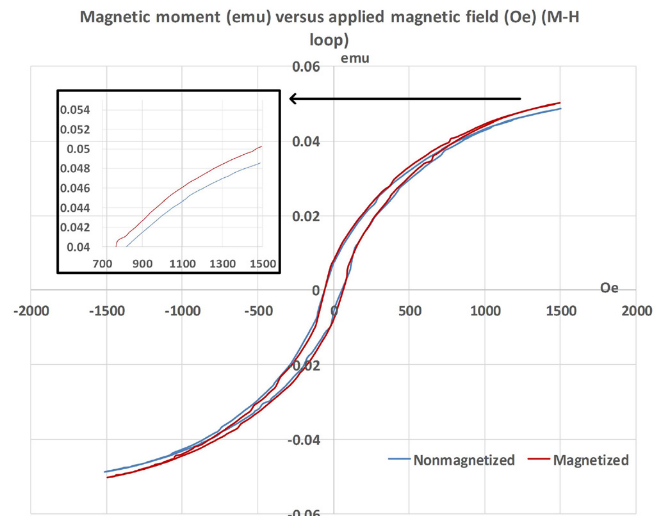

FIG. 6. Measured magnetization of a sample with and without magnetic annealing.

RIGHTSLINK

the alloy. In addition, the thermal expansion of plate and heater should be considered in the design to achieve higher temperatures. The heat transfer modelling in thin air gaps (100 nm) requires more detailed analysis to determine the dominant factors.

M. R. Yuce's work is supported by Australian Research Council Future Fellowships Grant FT130100430. This work was performed in part at the Melbourne Centre for Nanofabrication (MCN) in the Victorian Node of the Australian National Fabrication Facility (ANFF).

[1]N. V. Myung, D. Y. Park, B. Y. Yoo, and P. A. Sumodjo, J. Magn. Magn. Mater. **265**, 189 (2003).
[2]J. Y. Park and M. G. Allen, J. Micromech. Microeng. **8**, 307 (1998).
[3]M. T. Johnson, P. J. H. Bloemen, F. J. A. den Broeder, and J. J. de Vries, Rep. Prog. Phys. **59**, 1409 (1996).
[4]N. Lei, D. H. Wei, C. S. Tian, S. H. Xiao, D. Z. Hou, L. H. Zhou, and X. F. Jin, Appl. Phys. Lett. **95**, 192506 (2009).
[5]D. Chiba, S. Fukami, K. Shimamura, N. Ishiwata, K. Kobayashi, and T. Ono, Nat. Mater. **10**, 853 (2011).
[6]L. Thevenard, I. S. Camara, J.-Y. Prieur, P. Rovillain, A. Lemaître, C. Gourdon, and J.-Y. Duquesne, Phys. Rev. B **93**, 140405 (2016).
[7]M. Bagheri, M. Poot, M. Li, W. P. H. Pernice, and H. X. Tang, Nat. Nanotechnol. **6**, 726 (2011).
[8]G. Herzer, J. Magn. Magn. Mater. **254–255**, 598 (2003).
[9]R. B. Zmood, "Memory devices," U.S. patent 7,434,737 (2008).
[10]D. P. Arnold, S. Das, F. Cros, I. Zana, M. G. Allen, and J. H. Lang, J. Microelectromech. Syst. **15**, 406 (2006).
[11]E. Hashimoto, H. Tanaka, Y. Suzuki, Y. Uenishi, and A. Watabe, in *Proceedings of the IEEE Workshop on Micro Electro Mechanical Systems, 1994, MEMS'94* (1994) pp. 108–113.
[12]K. Wang, A. C. Wong, W. T. Hsu, and C. T. C. Nguyen, in *International Conference on Solid State Sensors and Actuators, TRANSDUCERS'97 Chicago* (1997), Vol. 1, pp. 109–112.
[13]A. Cowen, G. Hames, D. Monk, S. Wilcenski, and B. Hardy, *Metal-MUMPs Design Handbook* (MEMSCap Inc., 2011).

RIGHTSLINK